J Vis (2010) 13:17–23
DOI 10.1007/s12650-009-0007-4

REGULAR PAPER

Shuhei Fujimoto · Yuichi Murai · Yuji Tasaka · Yasushi Takeda

Visualization of transient interfacial waves induced by spin-up of two immiscible fluid layers

Received: 8 April 2009 / Revised: 9 July 2009 / Accepted: 25 August 2009 / Published online: 12 December 2009

Abstract Interfacial waves of two immiscible layers in a spin-up container were investigated using experimental visualization. While the interface near the central part rose up, instability waves propagated in an azimuthal direction on the interface. These waves were mainly caused by Kelvin–Helmholtz instability for the velocity difference between two layers during spin-up, but had complicated transient characteristics owing to the rotation in a closed system. We visualized the structure of the interfacial waves by the use of three types of optical characteristics of the interface. Image processing provided the detailed factors of the interfacial waves that were classified in four life stages from their generation to disappearance. The initial generation process involved many frequency modes due to a large velocity difference, and then a low mode stood out during the growth, and disappeared with an ellipsoidal sloshing mode to achieve the rigid rotation in both layers.

Keywords Interfacial wave · Instability · Two-layered flow · Rotating flow

1 Introduction

The flow in which the fluids are separated into different density layers is called stratified flow. Control of the interface between the layers has been an important problem in container engineering, and also has been a recent hot topic in micro-scale studies (Someya et al. 2003; Sugii et al. 2005). At the same time, spin-up of fluid has been a fundamental issue in fluid mechanics and has a long history of research from many aspects (Benton 1974; Duck and Foster 2001). The transient behavior of fluid arising from spin-up is associated simply with viscosity and density. Geophysical fluid dynamics addresses the issue that these properties vary in space. The finite volume of a single fluid in a rotating container has a high degree of unsteadiness on its boundary (Tasaka et al. 2008). When a cylindrical container filled with two liquids starts to rotate from rest, each phase displaces and begins to experience convection depending on the combination of two properties, and waves propagate on the phase interface. When there are two different immiscible fluids in the process, sharp changes in these properties on the interface provide various unpredictable nonlinear phenomena (Bonn et al. 2004). The interfacial motion is induced by centrifugal acceleration, and the motion alters the ambient fluid flow at the same time. This two-way interaction gets active for small differences in density and large differences in viscosity. Such an effect is seen in an oil–water combination as well as in a microgravity environment.

S. Fujimoto (✉) · Y. Murai · Y. Tasaka · Y. Takeda
Graduate School of Engineering, Hokkaido University, Kita-ku, Sapporo N13W8, Japan
E-mail: fujimoto@ring-me.eng.hokudai.ac.jp
Tel.: +81-11-7066373
Fax: +81-11-7067889

A large upheaval of the oil–water interface owing to spin-up has been investigated theoretically in the past (Berman et al. 1978; Lim et al. 1993; Kim and Hyun 1994). In the initial stage, bottom water rises up in the central container despite to our understanding of the rotation effect. This reversed deformation occurs owing to a viscosity difference beyond the interface, i.e. high-viscous oil rotates faster than water resulting in a large positive radial pressure gradient. In addition to this fact, the transient azimuthal waves travel on the interface during the upheaval process, which was partly reported by Berman (1978). The interfacial waves were ignored in many cases, however, strongly the interfacial area and thus the friction and the mass transfer were promoted. Some wave situations might cause large standing waves in resonance with the revolution of the container. The issue is when and how the waves are generated and grown during the spin-up. The principal reason for the generation should be the so-called Kelvin–Helmholtz instability for velocity and density differences between the two layers (Batchelor 1967). An alternative possible cause is the Holmboe instability (Holmboe 1962; Umurhan and Heifetz 2007) that happens to a thick boundary layer around the interface. These instabilities are, however, explained for two parallel fluid layers but not in a rotating flow. Moreover, the growing process has the unique mode of being different from linear instability analysis because of the circular closed system. Therefore, the configuration is totally different from dual parallel layers, and we need to observe carefully how the waves behave as a function of time in the confined space. In this paper, a series of visualized interfacial waves are shown and the underlying physics best suited to our understanding is described.

2 Visualization of interfacial deformation

Figure 1 shows a schematic diagram of the experimental setup. The cylindrical container was made of transparent acrylic resin with an internal diameter of 190 mm and a height of 350 mm. A stepping motor (Oriental Motor, MSM569-501K) was connected to the container to rotate it for the range of 0.64–19.46 rad/sec. The rotation speed was set at π rad/sec (30 rpm). The depths of the oil and water layers are 130 and 175 mm. The oil was silicone oil (Nippon Unicar, L45) of 100 cSt in kinematic viscosity. Digital video cameras (Panasonic, HDC-SD1-S) captured the motion of the interface at 30 fps from the top and the side of the container. To observe the interfacial waves from the top, two techniques were applied for capturing the complex interface based on the refraction of light at the interface and dye illumination in a sheet of light. The former approach utilized a color-stripe sheet of 190 mm in diameter placed on the container bottom. The color-stripe consisted of three primary colors: red, green, and blue assigned concentrically with radial intervals of 10 mm. The waves were detected on the captured image by the radial displacement of the stripe pattern (Fig. 1, middle). The displacement was provided by the refraction of light on the oil–water interface when it was inclined from the horizontal plane. The latter approach adapted a laser light sheet with a thickness of 4 mm (Kato Kouken, Green Laser Sheet 50m/G) from the side. The lower water was dyed by Sodium Fluorescein (Wako, Uranine 216-00102) to emphasize the interface between the two liquids. The waves were detected on the captured image by the radial displacement of the water layer (Fig. 1, right). With this method, the wave characteristics were obtained qualitatively for the wave amplitude, and quantitatively for the azimuthal wavenumber as well as wave frequency.

Figures 2 and 3 show the visualized images of the oil–water interface after the spin-up of the container at $t = 0$ s. As seen in Fig. 2, the bottom water layer rises in the central region as time elapses. This upheaval is caused by the oil layer with high viscosity being driven by the spin-up faster than the water layer. Thus, the oil layer produces a radial pressure gradient earlier than the water layer resulting in a convex interface against gravity. This time evolution of the interface can be theoretically predicted by the difference in momentum diffusion between the two layers and it has been investigated experimentally (Lim et al. 1993; Kim and Hyun 1994; Sugimoto and Iguchi 2002). During the upheaval process, the interfacial waves appear at $3.8 < t < 8.4$ s to form a jellyfish pattern.

Azimuthal distributions of the waves were visualized and are shown in Fig. 3. The number of waves and their amplitude change with time. A long time rotation makes the velocity difference between the two layers decrease, and hence the instability ceases to smooth the interface at $t > 20$ s. After the fine waves disappear, the swell of the interface reaches a maximum height at its center and has a parabolic shape. Careful observation of the shape shows that the interface involves ellipsoidal deformation that corresponds to the wave number of one. This mode is does not decayed quickly because it coincides with the natural sloshing frequency in the container (the theoretical description is omitted in this paper). The time evolution of the interfacial height on the central axis is shown in Fig. 4.

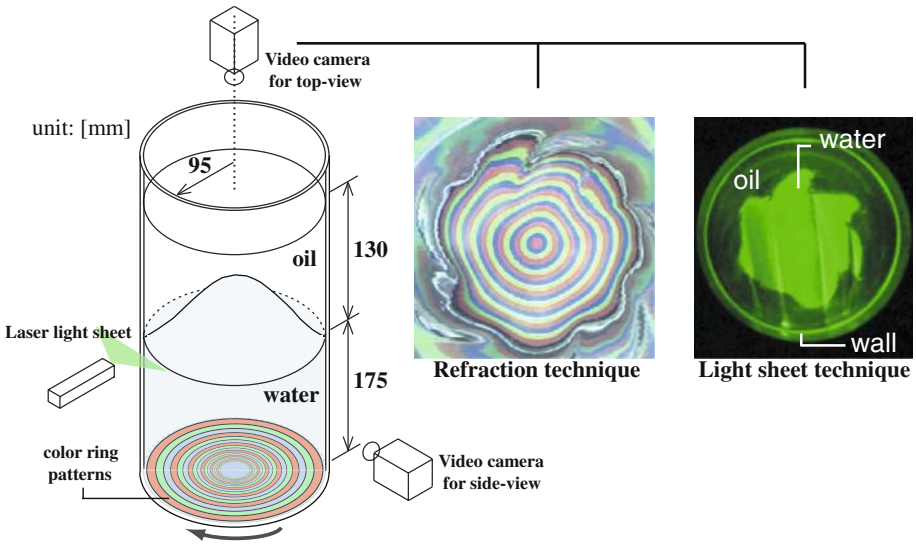

Fig. 1 Experimental configuration for three types of interfacial visualization

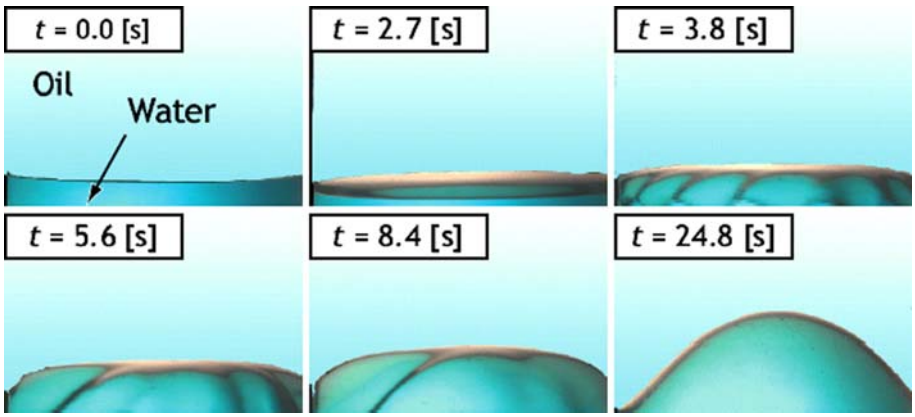

Fig. 2 Horizontal views of the interface upheaving with formation of azimuthal waves

The height reaches a peak around $t = 30$ s, and then decreases with time to be nearly zero at $t = 180$ s. The measured upheaval process corresponds to the theoretical estimation (Berman et al. 1978), which has a time scale longer than that of the interfacial waves. Thus, there are two different phenomena coupling each other in the cylinder. The interfacial waves, a focus of this study, are generated during the upheaval process. The characteristic spatio-temporal scales of the waves are hard to predict with linear theory of their interaction, particularly for a rotating system. The quantitative visualization allows us to deepen our understanding of the wave generation mechanism.

3 Propagation of the interfacial waves

3.1 Four life stages of the interfacial waves

In order to understand how the interfacial waves are generated, the time serial top-view images of the color ring patterns are converted to a single picture in a clock-type diagram as shown in Fig. 5. This conversion is performed for a line-sampled segmental image by integrating it in a time direction until the waves cease.

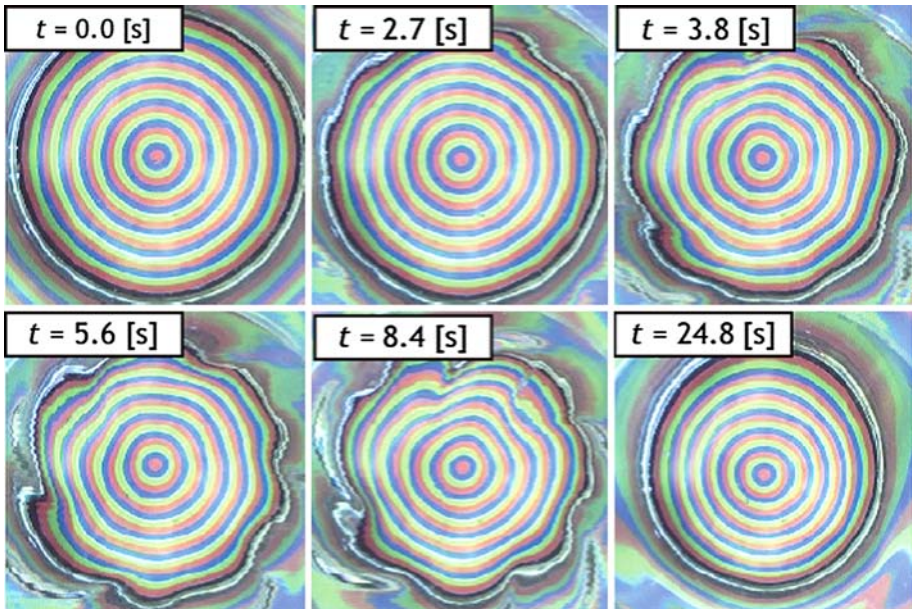

Fig. 3 Vertical views of azimuthal waves identified by the distortion in color ring patterns

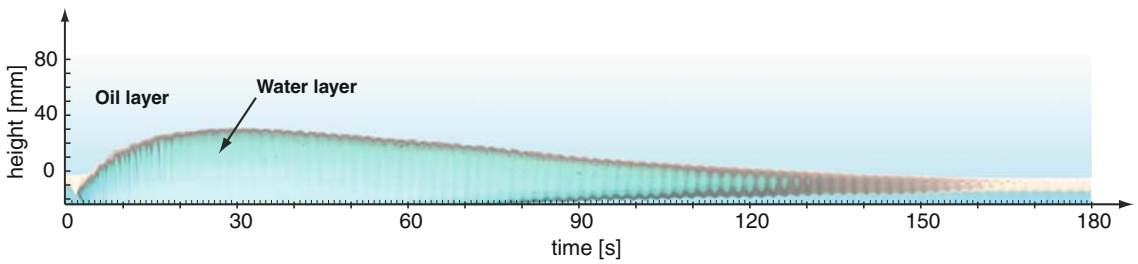

Fig. 4 Time evolution of the central height of the interface until reaching perfect rigid rotation

12 o'clock matches the dimensionless measurement time of $\Omega\, t/2\pi = 12$ (correspond to $t = 24$ s in Fig. 4). The radial coordinate corresponds to the actual radial position of the container.

With this expression, the four stages of the waves are identified. After a short time lag from the start of spin-up, the waves are generated from 1 to 2 o'clock, and grow from 2 to 5 o'clock. The number in the blue circle outside the clock indicates the number of the waves in an azimuthal direction obtained by Fourier analysis. The number of the waves starts from a large value due to abrupt driving of the fluid, which includes the harmonics of a base wave. It then decreases with the growth of the wave amplitude. A quasi-steady mode takes place from 5 to 8 o'clock, in which large waves at the wave number of four occupy the entire radius. After 8 o'clock, the waves are gradually damped except for the ellipsoidal sloshing mode that has a wave number of unity. We think that the down shifting of the wave number occurs for two reasons: one is because the rotational speeds of the two fluids are accelerated. During this acceleration, the shear rate around the interface is continuously decreasing. This will reduce the wave number on the interface as the flow is developed. Another factor is the confinement effect, i.e. instability waves are packed inside the cylindrical space. The development of a single wave interacts and coexists with other waves to produce a nonlinear interaction. The color stripe pattern at 12 o'clock shrinks relative to the initial pattern with a parabolic lift of the interface. Additionally, in our experiment, we observed the number of waves increase with increases in the rotational speed of the container. The maximum wave number at the generation stage is restricted by interfacial tension (which is around half of the air–water combination), however the wave behavior in the growth and quasi-steady stages is unaffected by the interfacial tension since the Weber number is estimated to be larger than 200.

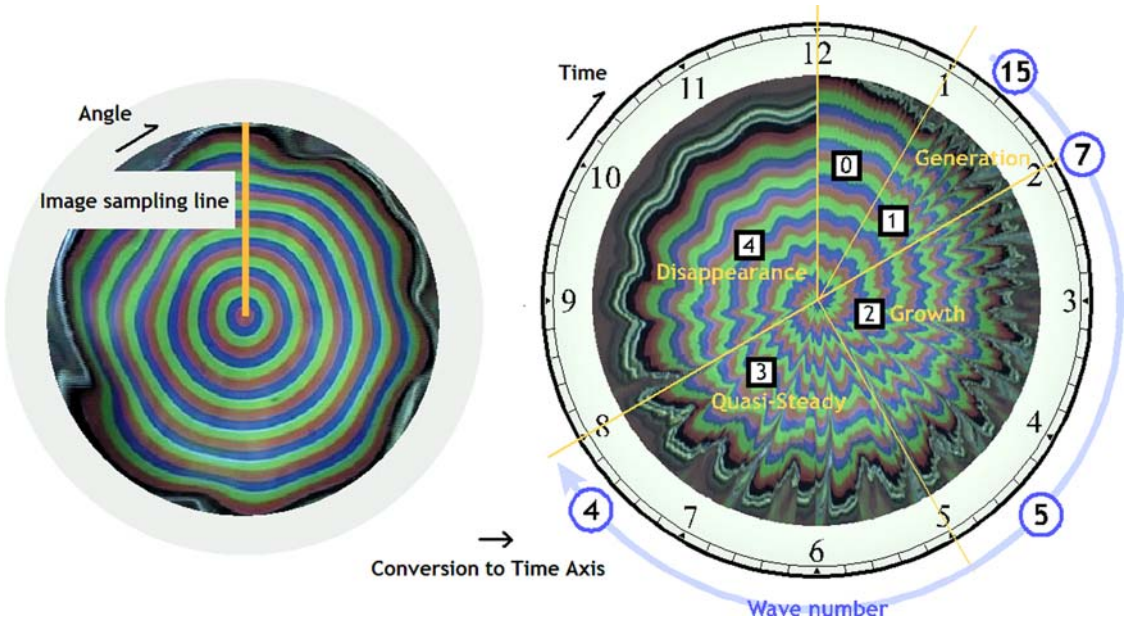

Fig. 5 Four life stages of interfacial waves distinguished using a clock diagram of the refraction image

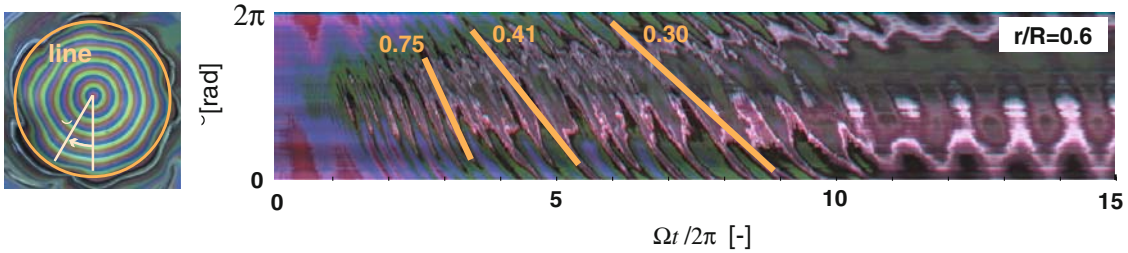

Fig. 6 Azimuthal propagation of waves visualized by circular image analysis

Figure 6 shows the similar conversion of the image for a circular sampling as shown in the left picture. This is therefore a time-angle 2-D visualization of the waves. The abscissa is non-dimensionalized by the rotational speed of the tank (the numeric of the axis means the number of rotations). Here, the sampling line is taken at $r/R = 0.6$, i.e. the most active region of the interfacial waves. The diagonal color patterns appearing in the map indicate the propagation of the interfacial waves in the azimuthal direction. Since the camera rotates together with the container, the waves propagate toward a negative angle because of the waves traveling slower than the container's angular velocity in absolute coordinates. As highlighted by the three slopes in yellow, the dimensionless traveling speed starts from unity during the wave's growth, and decreases gradually with time. The three dimensionless traveling speeds are approximately 0.75, 0.41, and 0.30. This implies that the initial rotation of the waves originate only from the oil layer of high viscosity when water convection is inactive. After the two layers are accelerated, in keeping a certain velocity difference, the waves grow up in the manner of the Kelvin–Helmholtz instability to have an intermediate traveling speed less than unity.

3.2 Three-dimensional structure

Due to large upheaval displacement of the interface, the waves actually show three-dimensional behavior that varies with time. For instance, the waves interact with centrifugal acceleration that has a gap between the two liquids at different velocities. This will push the selected waves in a radial direction to provide an asymmetric wave form.

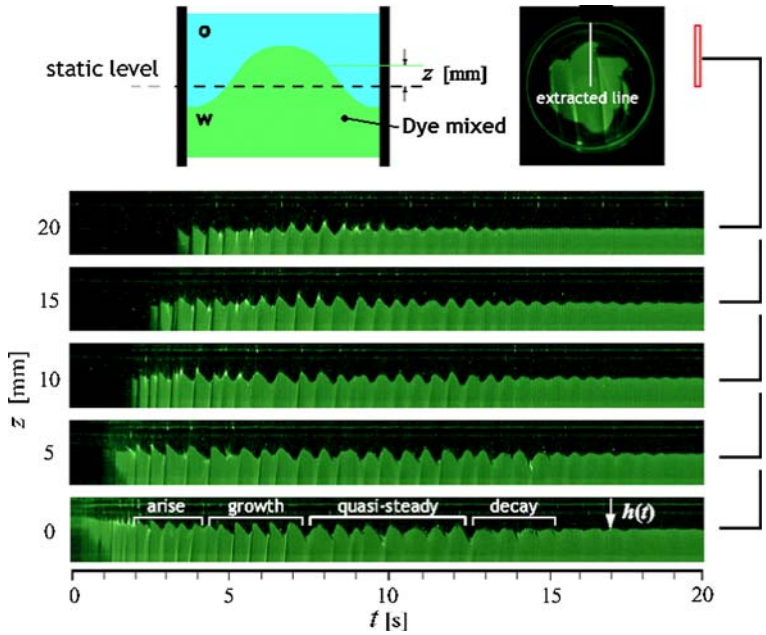

Fig. 7 Four life stages of interfacial waves distinguished with a clock diagram of the refraction image

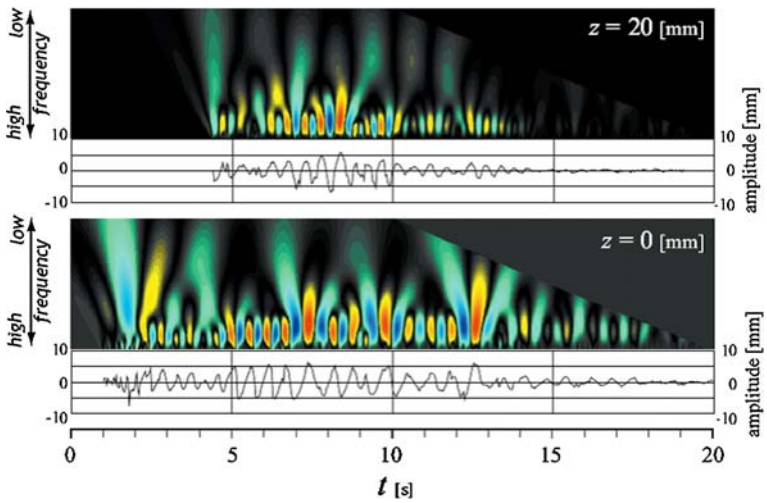

Fig. 8 Wavelet analysis of interfacial wave behavior to identify interaction among waves

Figure 7 shows the laser light visualization images on five different horizontal planes as a function of the height z ($z = 0$ means the height of the interface at the rest state). The radial position of the interface is visualized with the contrast between the two layers. The temporal behavior of the wave can be quantitatively investigated by the conversion of the image into spatio-temporal 2-D images. Expressing the displacement of the interface by $h(t)$ as shown in the figure, a wavelet approach is employed to evaluate how these waves interact with others in a closed system.

Figure 8 shows the wave forms of $h(t)$ and the results of the continuous wavelet transform. Here, the Mexican hat function is adopted as a mother wavelet. The color indicates the wavelet coefficients, i.e. the correlation between $h(t)$ and the mother wavelet. Because of space limitations, two results measured at $z = 0$ and $z = 20$ mm are shown to discuss the three-dimensionality of the wave behavior. At $z = 0$ mm, the interfacial wave starts to occur in a wide frequency band. This is explained by the stepwise acceleration

of the velocity difference that involves a broad spectrum in frequency space. During the wave generation stage for $t < 5$ s, waves of a high frequency mode are induced owing to the large velocity difference maintained between the two layers. In the quasi-steady stage at $5 < t < 12$ s, the primary frequency shifts to a lower frequency similar to the spatial development of Kelvin–Helmholtz instability waves in two-layer parallel flows. The difference from parallel flows is that these waves circulate in the azimuthal direction in a closed container. This confinement provides interaction among waves as seen by the cyclic burst of the wavelet coefficient to a lower frequency. The burst originates from the blue event in the figure, and thus has a negative coefficient. This corresponds to radial outward ejection of the water layer from selected waves. Phenomenological similar events are known in Taylor–Couette flow on a modulated wavy vortex mode (Nomura et al. 2008). The underlying physics might have the same root. Here, spatial development of flow instability or flow transition is being packed in a closed system. By contrast, in the wavelet's result at the top of the upheaval, $z = 20$ mm, the wave mode is higher in frequency than that at the foot. This means that the waves rotate faster near the top than the foot to form a free-vortex type of traveling wave. The coexistence of these different waves in the single closed system is the most notable feature of the present flow configuration.

4 Summary

We studied the interfacial waves induced by the spin-up of two immiscible liquids. The waves occur due to the initial velocity difference between the two layers, i.e. the Kelvin–Helmholtz instability. This is different from that in a parallel two-layer flow where the instability waves circulated in a closed system resulting in interaction between them. The color-ring visualization based on the light refraction technique shows the four life stages of the interaction from the generation of waves to their disappearance. In particular, we focus on the standing waves that propagate in the azimuthal direction during the upheaval of the bottom layer by means of laser sheet visualization combined with the wavelet approach. This quantitative visualization leads to an understanding of the coexistence of different waves packed in the single space and also deepens the discussion on the modulation of the waves due to their interaction. The present paper deal with a specific case picked up from a variety of two-layer interactions, however, the process of visualization explored the interesting physics underlying a rotating system. In fact, the technique is useful, in principle, for designing new phase-mixing/separation, interfacial area control, and for the use of nonlinear wave interaction in the future.

References

Batchelor GK (1967) An introduction to fluid dynamics. Cambridge University Press, London
Benton ER, Clark A (1974) Spin-up. Annu Rev Fluid Mech 6:257–280
Berman AS, Bradford J, Lundgren TS (1978) Two-fluid spin-up in a centrifuge. J Fluid Mech 84:411–431
Bonn D, Kobylko M, Bohn S, Meunier J, Morozov A, van Saaloos W (2004) Rod-climbing effect in Newtonian fluids. Phys Rev Lett 93:214503
Duck PW, Foster MR (2001) Spin-up of homogeneous and stratified fluids. Annu Rev Fluid Mech 33:231–263
Holmboe J (1962) On the behavior of symmetric waves in stratified shear layers. Geofysiske Publikasjoner 24:67–113
Kim KY, Hyun JM (1994) Spin-up from rest of a two-layer liquid in a cylinder. J Fluid Eng 116:808–814
Lim TG, Choi S, Hyun JM (1993) Transient interface shape of a two layer liquid in an abruptly rotating cylinder. J Fluid Eng 115:324–329
Nomura Y, Tasaka Y, Murai Y, Takeda Y (2008) The behavior of Couette–Taylor flow in an azimuthal plane. J Phys Conf Ser 137(012001):1–6
Someya S, Munakata T, Nishio M, Okamoto K (2003) Preliminary study of two immiscible liquid layers subjected to a horizontal temperature gradient. J Visual 6:21–30
Sugii Y, Okamoto K, Hibara A, Tokeshi M, Kitamori T (2005) Effect of Korteweg stress in miscible liquid two-layer flow in a microfluidic device. J Visual 8:117–124
Sugimoto T, Iguchi M (2002) Behavior of immiscible two liquid layers contained in cylindrical vessel suddenly set in rotation. ISIJ Int 42:338–343
Tasaka Y, Ito K, Iima M (2008) Visualization of a rotating flow under large-deformed free surface using anisotropic flakes. J Visual 11:163–172
Umurhan OM, Heifetz E (2007) Holmboe modes revised. Phys Fluids 19:064102